

# Procedural Noise Adversarial Examples for Black-Box Attacks on Deep Neural Networks

Kenneth T. Co  
Imperial College London  
kenneth.co16@imperial.ac.uk

Luis Muñoz-González  
Imperial College London  
l.munoz@imperial.ac.uk

Emil C. Lupu  
Imperial College London  
e.c.lupu@imperial.ac.uk

## ABSTRACT

Deep Neural Networks (DNNs) have been shown to be vulnerable to adversarial examples – perturbed inputs specifically designed to produce intentional errors in the learning algorithms at test time. Various white-box attacks have proven the fragility of DNNs against adversarial examples. However, existing black-box attacks are either computationally expensive or require extensive knowledge of the target model and its dataset to succeed. Thus, such methods are not practical in a concrete setting. In this paper we introduce a more structured approach for generating adversarial examples in computer vision problems based on the use of procedural noise patterns. Our approach unveils a systemic vulnerability of DNNs to such patterns in this application domain. We further demonstrate that it is possible to construct practical black-box attacks with low computational cost and a reduced number of queries against robust architectures such as Inception v3 and ResNet v2 on the ImageNet dataset. We propose to use Bayesian optimization to efficiently learn the parameters that control the structure of the adversarial noise patterns. Using such an approach our black-box attack outperforms existing white and black-box attacks against ImageNet. We also evidence the limitations of adversarial training: the attacker just needs to change their perspective to generate the adversarial examples to bypass the defence and craft successful attacks, whereas, for the defender, it is difficult to foresee all possible types of adversarial perturbations. Finally, and more worryingly, we show that our procedural noise perturbations are “universal” and “transferable” in that they generalize across different inputs and models respectively. This finding may give insight on the nature of transferable and universal adversarial perturbations.

## CCS CONCEPTS

•Computing methodologies → Machine learning; •Security and privacy → Usability in security and privacy;

## KEYWORDS

Adversarial examples; Bayesian optimization; black-box attacks; computer vision; deep neural networks; procedural noise

## 1 INTRODUCTION

Advances in computation and machine learning have allowed deep neural networks (DNNs) to become the favoured algorithm in machine learning for various tasks such as computer vision [28], malware detection [58], playing games [61], and speech recognition [19]. DNNs achieve human-like or better performance in some of these applications. Given their increased use in safety-critical and security applications such as autonomous vehicles [6, 68, 70], intrusion detection [20, 24, 25], malicious string detection [59], and facial

recognition [34, 64], it is important to ensure that such algorithms are robust to malicious adversaries. Yet despite the prevalence of neural networks, their vulnerabilities remain poorly understood.

It has been shown that machine learning systems are vulnerable to attacks [2, 21, 36, 42, 50] performed both at training time and at test time. In training, the attacker can craft *poisoning attacks* by injecting malicious data into the training dataset to subvert the model’s learning algorithm and degrade its performance [5, 15, 26, 27, 37, 43, 44, 51, 52]. At test time, the attacker can exploit weaknesses of the learning algorithm to produce intentional errors. These are commonly referred to as *evasion attacks*.

For evasion attacks, neural networks have been shown to be susceptible to *adversarial examples*: inputs indistinguishable from genuine data points but designed to be misclassified by the learning algorithm [67]. As the perturbation required to fool the learning algorithm is usually small, detecting adversarial examples is a challenging task. Fig. 1 shows an adversarial example generated with the attack strategy we propose in this paper; the perturbed image of a tabby cat is misclassified as a shower curtain. Although we focus on image classification, this phenomenon is not restricted to computer vision and adversarial examples have been shown in speech processing [8, 11], malware classification [17], and reinforcement learning [22, 33], among others.

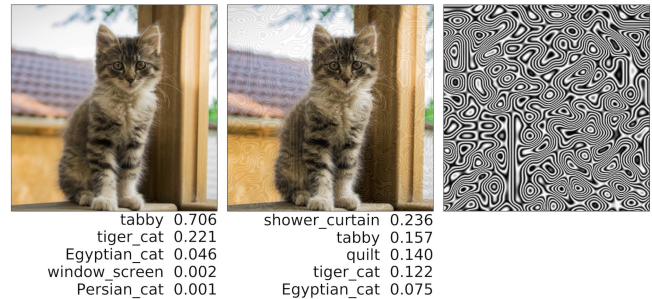


**Figure 1: Adversarial example generated with a procedural noise function. From left to right: original image, adversarial example, and procedural noise (magnified for visibility). Below are the classifier’s top 5 output probabilities.**

Attack strategies that craft adversarial examples have been proposed in both white and black-box settings, making different assumptions on the adversary’s knowledge and capabilities [50]. The more successful white-box algorithms generate adversarial examples with gradient-based optimization<sup>1</sup> and differ in their optimization objectives [4, 10, 16, 29, 35, 41, 49, 67]. Though effective, many

<sup>1</sup>Gradient-based methods rely on the computation of gradients to generate adversarial examples.

of these attacks require full white-box access to the target model, which is not always feasible in real world settings.

Black-box attacks usually adopt one of two approaches: either, by exploiting the transferability property<sup>2</sup> of adversarial examples [47], or, by estimating the gradient of the objective function for the attacker [12, 23]. The former method requires a model that is similar to the target and trained on a similar dataset while the latter method requires many queries and does not scale to natural large-image datasets, such as *ImageNet* [57], where approximations to the DNNs loss are applied to produce adversarial examples [30, 69].

In this paper, we propose a novel approach for generating adversarial examples using procedural noise in restrictive black-box settings i.e., where only query access is available and no knowledge of the target classifier or its training dataset are assumed. Procedural noise functions are used in computer graphics and designed to be parametrizable, fast, and lightweight [31]. Their primary purpose is to algorithmically generate textures and patterns and they have common applications in motion pictures and video games. The ability of procedural noise to generate high frequencies of curves and edges, similar to current adversarial examples, initially prompted our approach.

We empirically demonstrate that DNNs are fragile to *procedurally generated noise* across several metrics. Our experimental results for the large-scale *ImageNet* dataset on Inception classifiers show that our proposed black-box attack achieves up to 80% success. We also tested our attack against adversarially trained models [35, 67, 69], i.e. where adversarial examples are added to the training dataset [1]. Although adversarial training has been effective to defend against gradient-based attacks, we show that it does not greatly diminish the impact of our procedural noise perturbations. We also observe that procedural noise exhibits properties of *universal adversarial perturbations* [41] that can fool the classifier across a large fraction of the dataset. These raises the potential for large-scale black-box attacks against neural network-based image classification systems.<sup>3</sup>

Our contributions in this paper include:

- We introduce a novel and intuitive black-box attack against DNNs for image classification using procedural noise functions. Our attack leverages the capabilities of procedural noise functions to generate parametrizable textures in a scalable and computationally efficient way.
- We empirically show that our method achieves comparable performance with existing white-box algorithms for generating fast adversarial examples and up to twice the performance of black-box transfer attacks, both of which require stronger adversaries than our attack.
- We observe that our procedural noise adversarial examples generalize across images and classifiers—with single procedural noise perturbations able to cause classifier error on at least 40% across 4 robust classifiers. To our knowledge, ours is the first model-agnostic black-box generation of universal adversarial perturbations.

<sup>2</sup>Adversarial examples that are successful against one machine learning model are often successful against similar models.

<sup>3</sup>We have also successfully tested our attack on real image classification services and have disclosed our results to the providers of those services. We are still waiting for their consent to include the results in this paper.

- We show that the state-of-the-art *ensemble adversarial training* [69] defence does not significantly diminish the effect of procedural noise perturbations. Testing of robust defences must therefore also incorporate attacks other than gradient-based optimization techniques.
- We demonstrate that our attack can be used as a query-efficient black-box attack, achieving 81.3% of state-of-the-art performance with only 3.2% of the queries, effectively improving the efficiency 25 fold.
- We propose *Bayesian optimization* [39, 63] as an effective tool for black-box attacks, showing that it improves our attack’s query efficiency by up to 52.4% on average when compared to random search. This is desirable for attackers with restricted access or query budgets to the target model.

The rest of this paper is structured as follows. In Sect. 2, we define a taxonomy to evaluate evasion attacks. In Sect. 3, we describe and motivate the use of procedural noise to generate adversarial examples. In Sect. 4, we describe a detailed implementation of our procedural noise attack. In Sect. 5, we define our experimental setup. In Sect. 6, we analyze our attack’s performance and compare it to existing work. In Sect. 7 we discuss our results, limitations, potential defences, and how our attack can be extended to other applications. Finally in Sect. 8 we summarize our findings and suggest future research directions.

## 2 ATTACK TAXONOMY

This study focuses on attacks during test time, also known as evasion attacks. To determine the viability of attacks in practical settings against natural datasets, we evaluate and compare them based on two primary factors: (a) their effectiveness and (b) the access and knowledge the adversary requires. In this section, we outline a taxonomy to develop this idea. Other limitations such as computation speed or computing power are relevant, but difficult to categorize across applications as computing power can vary greatly.

### 2.1 Effectiveness

The effectiveness or performance of an attack refers to its ability to degrade a model’s accuracy. At test time this means crafting inputs that the target model misclassifies, creating a denial of service or affecting the integrity of the model. We describe three metrics that can be used to evaluate an attack’s performance: its general score, transferability, and universality.

The **general score** of an attack is the error of the model across all adversarial examples, where the attack generates an adversarial example given a clean input. **Transferability** is when the same adversarial example can fool multiple classifiers [47]. This property enhances the strength of the attack as it can generate a single adversarial input to degrade the performance across multiple models. **Universality** is when the same adversarial perturbation can be applied across a large proportion of the input dataset to fool a classifier [40]. There is also *cross-model universality* which is a combination of transferability and universality, i.e. the adversarial perturbation generalizes across a large proportion of the input dataset and multiple classifiers. Satisfying this last property is a strong indicator of the attack’s generalizability.

## 2.2 Threat Model

The adversary’s knowledge and capabilities are on a spectrum from zero access and knowledge to complete control of the target model. For evasion attacks, existing work can be broadly classified into three categories: white-box, partial black-box, and restrictive black-box [50]. For these scenarios, we assume that the adversary cannot modify the model, but knows that it’s a neural network and has the ability to access model input and output. The adversary’s knowledge and access to the target model and its dataset will vary.

In **white-box** settings, the adversary has complete knowledge of the model architecture, weights, and training data. This is the scenario for the current state-of-the-art gradient-based attack [10, 16, 29, 35, 41, 67]. In **partial black-box** settings, the adversary is able to build a surrogate neural network of similar scale and has access to training data that is similar to that of the target model. This is the case for transfer attacks where white-box adversarial examples are generated on a surrogate model to attack the targeted black-box model [30, 48]. In a **restrictive black-box** setting, the adversary has no knowledge of the target model’s architecture, weights, or datasets and no access to surrogate datasets or models that are similar to the target’s.

For restrictive black-box adversaries, it is desirable to be *query-efficient* in that successful adversarial examples are generated with as few queries to the target model as possible. This is to reduce the query budget needed by the attacker, e.g. if querying the target model is a paid service, and to avoid detection from the defender by lowering the volume of suspicious queries. Existing restrictive-black box attacks like [3, 12] have shown some success with zeroth order optimization and gradient estimation, however these require tens or hundreds of thousands of queries on realistic natural-image dataset like ImageNet [13, 23]. The most query-efficient method so far is a bandit optimization framework that achieves 92.9% attack success with an average of a thousand queries per image on ImageNet [23]. These existing methods still require a large number of queries per image, which makes them impractical in real world settings.

## 3 PROCEDURAL NOISE

We introduce an intuitive approach for generating adversarial examples in a restrictive black-box setting with *procedural noise functions*. Current gradient-based methods find adversarial examples by incrementally traversing the classifier’s decision boundary based on assumptions and knowledge of the target model. In contrast, our approach explores a class of noise patterns that are for generating “natural” textures in computer graphics. This provides novel insights on the behaviour of neural networks in response to perturbations.

Procedural noise functions are procedural techniques used for generating image patterns. The term “procedural” refers to the noise being generated algorithmically. These noise functions are widely used in computer graphics and have numerous applications in film and video game production [31] amongst others. They are used to generate textures for the creation of natural details to enhance images. Specific examples include textures for glass, wood, marble, and animations such as cloud, fire, and ripple effects.

Given these properties, we hypothesize that procedural noise perturbations added to benign images can fool image classification

algorithms. The neural network’s max pooling and convolutional layers are generally able to filter out high-frequency noise, patterns that are visually noisy and not smooth. However, structured noise patterns that have high amounts of edges and shapes are more difficult for the network to ignore.

Procedural noise functions are designed to scale to large dimensions, be fast to evaluate, and have low memory footprints. They are also parametrizable, allowing the generation of different noise patterns from the same function. These attributes allow them to be used for computationally inexpensive black-box attacks as we will discuss below. For a more comprehensive survey on procedural noise, we refer the reader to [31].

### 3.1 Motivation

Current methods generate adversarial examples using gradient-based optimization such as in Carlini and Wagner’s attack [10], DeepFool [41], and Fast Gradient Sign Method (FGSM) [16]. They craft perturbations given white-box access and knowledge of the target classifier. The resulting appearance of their adversarial perturbations exploits some geometric correlations within the classifier’s decision boundaries [41], as the attacks directly leverage knowledge of the classifier’s weights to craft adversarial examples. We postulate that such vulnerabilities could be exploited with noise that shares its appearance.

We further observed that Universal Adversarial Perturbations (UAPs) from existing attacks appear to have visually noticeable structures in their perturbations. UAPs in particular are intriguing because they are designed to evade a classifier across multiple images using a single adversarial perturbation. Procedural noise, as shown in the third row of Fig. 2, appears to generate images somewhat similar to these UAPs. Thus, we decided to investigate whether procedural noise patterns have similar properties to UAPs, allowing attacks where a single perturbation achieves misclassification on a large proportion of images in a given set.

### 3.2 Types of Noise Functions

Procedural noise functions can be classified into three categories: lattice gradient noise, sparse convolution noise, and explicit noise [31]. **Lattice gradient noise** is generated by interpolating random values or gradients at the points of an integer lattice, with Perlin noise as a representative example. **Sparse convolution noise** is a sum of randomly positioned and weighted kernels,<sup>4</sup> with Gabor noise as a representative example. **Explicit noise** is different from the others in that the images are generated in advance and stored later for retrieval. Though the construction of explicit noise is not strictly procedural, it is relevant to computer graphics with Anisotropic and Wavelet noise as representative examples. Explicit noise is not used in this paper as it induces a large memory cost from its reliance on the storage and retrieval of pre-computed images [31]. This limits its feasibility as an inexpensive attack, and is why we leave this for future work.

### 3.3 Lattice Gradient Noise

We use the representative example, Perlin noise, because of its ease of use, popularity, and simplicity. Perlin noise was developed

<sup>4</sup>A kernel in image processing refers to a matrix used for image convolution.

as a technique to produce natural-looking textures for computer graphics, with its initial application in motion pictures, and it has remained a staple in the industry [31]. Although Perlin noise may not be the most expressive noise function, it has a simple implementation which makes it suitable for inexpensive black-box attacks as it only has a few parameters.

We summarize the formal construction of two-dimensional Perlin noise as described in [53–55]. The value at a point  $(a, b)$  is derived in the following way: Let  $(i, j)$  define the four lattice points of the lattice square where  $i = \{|a|, |a| + 1\}$  and  $j = \{|b|, |b| + 1\}$ . The four gradients are given by  $g_{ij} = \mathbf{V}[\mathbf{Q}[Q[i] + j]]$  where pre-computed arrays  $\mathbf{Q}$  and  $\mathbf{V}$  contain a pseudo-random permutation and pseudo-random unit gradient vectors respectively. The four linear functions  $g_{ij}(a - i, b - j)$  are then bilinearly interpolated by  $s(a - |a|)$  and  $s(b - |b|)$ , where  $s(t) = 6t^5 - 15t^4 + 10t^3$ . The result is the Perlin noise value  $p(a, b)$  for coordinates  $(a, b)$ .

The Perlin noise function has several parameters that determine the visual appearance of the noise. In our implementation, the frequencies  $v_a, v_b$  and number of octaves  $\omega$  contribute to the most visual change, so we focus on these parameters. Frequency corresponds to the rate of change between adjacent pixel values, it affects how visually smooth the image is. The number of octaves refers to the number of additional noise signals added onto the image where the next signal’s frequency is double the previous signal’s. Increasing this makes the visual appearance more detailed. The resulting gradient noise value at point  $(a, b)$  with parameters  $\theta_{\text{LGrad}} = \{v_a, v_b, \omega\}$  becomes

$$S_{\text{LGrad}}(a, b) = \sum_{n=1}^{\omega} p(a \cdot v_a 2^{n-1}, b \cdot v_b 2^{n-1})$$

### 3.4 Sparse Convolution Noise

We use the representative example, Gabor noise, because it has more accurate spectral control over other procedural noise [32]. Spectral control refers to the ability to control the appearance of noise as measured by its energy along each frequency band. The improved spectral control of Gabor noise is because it can be quickly evaluated at any point in space while being described by only a few parameters such as orientation, frequency, and bandwidth [32].

Gabor noise is generated by the sparse convolution of the Gabor kernel. The Gabor kernel  $g$  for parameters  $\{\kappa, \alpha, v, \omega\}$  is the product of a circular Gaussian and a harmonic function,

$$g(a, b) = \kappa e^{-\pi \alpha^2 (a^2 + b^2)} \cos [2\pi v(x \cos \omega + y \sin \omega)]$$

where  $\kappa$  and  $\alpha$  are the magnitude and inverse width of the Gaussian respectively, and  $v$  and  $\omega$  are the frequency and orientation of the harmonic respectively [31]. The value  $S(a, b)$  at point  $(a, b)$  is the sparse convolution noise with a Gabor kernel,

$$S_{\text{SConv}}(a, b) = \sum_{i=1}^N w_i g(a - a_i, b - b_i; \kappa, \alpha, v, \omega)$$

where  $\{(a_i, b_i)\}_i$  are random points,  $\{w_i\}_i$  are random weights, and  $N$  is the number of random points [31].

To make the search for adversarial perturbations computationally tractable, we restrict the random points to be integers uniformly drawn from  $a_i, b_i \in [0, 23] \cap \mathbb{Z}$ , which is common in code implementations, and weights to be uniformly drawn from the interval

$w_i \in (-1, 1)$ . We also fix the parameters  $\{\alpha, v, \omega\}$  for all  $i$  and set  $\kappa = 1$  to generate a subset of Gabor noise. By adding these constraints, we reduce the number of adjustable parameters at the expense of noise complexity. This trade-off is necessary for a black-box attack with a limited number of queries, as the higher number of parameters will make searching for adversarial perturbations more computationally difficult and possibly intractable.

The resulting sparse convolution noise value at point  $(a, b)$  with parameters  $\theta_{\text{SConv}} = \{N, \alpha, v, \omega\}$  is given by  $S(a, b)$  with the above constraints for random  $a_i, b_i$ , and  $w_i$ .

### 3.5 Colour Maps

Colour maps are used to create additional variation in the appearance of the image. An example of how the colour map affects the visual appearance can be seen in Fig. 2. To achieve patterns with many edges, we use a sine function with a frequency parameter  $v_{\text{sine}}$ . We define this for the noise value  $q$  with the function  $C(q) = \sin(q \cdot 2\pi v_{\text{sine}})$ . The periodicity of the sine function creates distinct bands in the image to achieve a high frequency of edges.

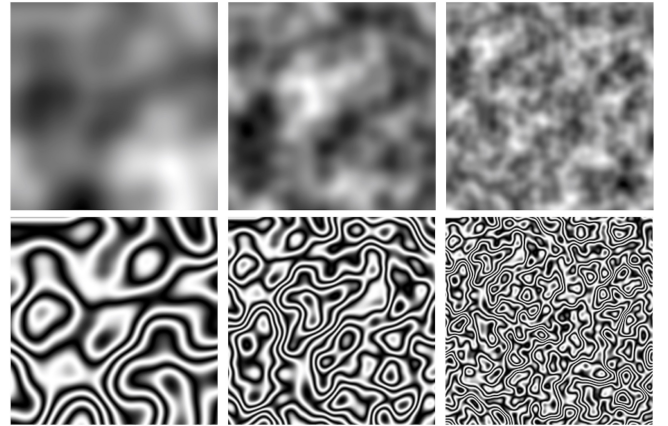


**Figure 2: Samples of lattice gradient noise with colour maps: (top) greyscale and (bottom) greyscale sine function.**

We choose a greyscale colour map, i.e. the three channel values (red, green, blue) are the same, to reduce the complexity of our function. Sacrificing noise complexity allows us to have a more tractable search space for potential adversarial examples as we have fewer parameters. This trade-off is necessary for a black-box attack with a limited number of queries, similar to the reasoning made when restricting the type of sparse convolution noise.

The noise generating function  $G$  at point  $(a, b)$  can be defined as the composition of our procedural noise function and greyscale sine colour map,

$$G(a, b) = C(S(a, b)) = \sin((S(a, b) \cdot 2\pi v_{\text{sine}}))$$

For each procedural noise function, the combined parameters are  $\theta_{\text{LGrad}} = \{v_a, v_b, \omega, v_{\text{sine}}\}$  and  $\theta_{\text{SConv}} = \{N, \alpha, v, \omega, v_{\text{sine}}\}$  for  $G_{\text{LGrad}}$  and  $G_{\text{SConv}}$  respectively.

This parametrizable property of our noise function greatly reduces the search space for adversarial perturbations. Instead of

searching over the entire image space like in gradient based methods, which can be up to 268,203 pixels for ImageNet, we optimize over a significantly smaller space of 4 to 5 parameters. This large reduction in the number of features improves the scalability and speed of the attacks given a restrictive black-box setting.

## 4 ATTACK

Our proposed attack is a query-based black-box algorithm that leverages the properties of procedural noise. A summary of our attack algorithm is as follows: having chosen a noise generating function  $G$  with parameters  $\theta$ , we create an image perturbation to add to the original image. The target model will then be queried with this altered image. If the attack is unsuccessful, we update our subsequent query parameters  $\theta$  randomly or with Bayesian optimization aiming to optimize the attacker’s objective function.

### 4.1 Formal Threat Model

We formalize the construction of adversarial examples as an optimization problem, following the structure used in [10, 41, 67]. We also formalize the restrictive black-box threat model outlined in Sect. 2.2 by describing our attack in terms of the adversary’s goal, knowledge, and capabilities. This is a general framework that can be used for applications outside of computer vision.

*Notation.* Given a multi-class classification problem with  $k$  classes and a learned classifier  $F$ , let  $F(x)$  be its output probability scores for an input  $x$ . Thus,  $F(x)$  is a  $k$ -dimensional probability vector, where  $F_i(x)$ , the  $i$ -th element in  $F(x)$ , represents the probability that  $x$  belongs to class  $i$ .<sup>5</sup> When there are a large number of classes (for example ImageNet dataset has 1,000 class labels) the performance of a classifier is measured by its “top  $n$ ” accuracy, i.e. when the correct label is among the  $n$  highest probability scores. Let  $T_n(x)$  be the  $n$ -th highest probability score given input  $x$ . When  $n = 1$ , we have  $T_1(x) = \arg \max_i F_i(x)$ , which is the classifier’s predicted label for  $x$ . Let  $\tau(x)$  denote the true label of object  $x$ . **Top  $n$  error** occurs when  $F_{\tau(x)}(x) < T_n(x)$ , the probability for the true label is not within the top  $n$  scores. Let  $G$  be the adversary’s chosen generating noise function and  $\theta$  be its parameters. For shorthand, we define  $G(\theta)$  as the resulting adversarial perturbation, i.e. the function  $G$  applied to each pixel coordinate to generate an entire image. We denote the adversarial example  $x'$  to be the sum of the input  $x$  and the generated adversarial perturbation  $G(\theta)$ , i.e.  $x' = x + G(\theta)$ .

**Adversary Knowledge.** The targeted model is a black-box classifier that has completed learning and is accepting input queries. We assume the adversary has no insider knowledge of the target classifier such as its learning algorithm, training data, and model settings. Although the adversary knows the data types of the classifier’s input, output, and class labels.

**Adversary Capabilities.** The adversary can query the target classifier  $F$  with any input  $x$  and knows the true class labels  $\tau(x)$  for these inputs. In some cases, image classifiers provide the probability vector as an output, to show the classifier’s confidence and the alternative predictions. It is therefore plausible that the adversary can observe the output class probabilities  $F(x)$ . We also consider the case where this probability output vector is not available.

<sup>5</sup>Note that  $\sum_{i=1}^k F_i(x) = 1$ .

**Adversary Goals.** Given legitimate inputs, the adversary wants to produce top  $n$  error in the target classifier given budget on how they can modify the original input. The primary goal of the adversary is to achieve misclassification by reducing the probability of the true class label  $F_{\tau(x)}(x')$  for adversarial example  $x'$ . This is trivial when the genuine input  $x$  is already misclassified. We also focus on indiscriminate rather than targeted misclassification, although our methodology can be applied to both.

Constraints on the maximum allowable modification are defined in terms of some distance metric  $d(x, x')$  between the original input  $x$  and the adversarial input  $x'$ . In computer vision, this is equivalent to limiting the norm<sup>6</sup> of the perturbation  $\|G(\theta)\| < \epsilon$  for some  $\epsilon > 0$ . This is to preserve the true label of the adversarial example. We also include a limit on the number of queries  $q_{\max}$  as too many queries becomes impractical and risks the attack being discovered.

### 4.2 Objective Function

We can now define the constrained optimization problem for generating adversarial examples. Given a learned classifier  $F$  with  $k$  classes, the adversary has an input  $x$  that they want to alter, so that the new input  $x' = x + G(\theta)$  is top  $n$  misclassified by  $F$ , with constraints on the distance  $\|G(\theta)\| < \epsilon$  and the number of queries  $q < q_{\max}$ .

In line with related work, we assume that our perturbation budget  $\epsilon$  is small enough so that it visually preserves the original label  $\tau(x') = \tau(x)$  for any generated  $x' = x + G(\theta)$ . The algorithm’s goal is to optimize our chosen generating function  $G$  over the parameters  $\theta$ . Top  $n$  error occurs when  $F_{\tau(x')}(x') < T_n(x')$  so the optimization problem can be formulated as follows:

$$\begin{aligned} \min_{\theta} \quad & F_{\tau(x)}(x + G(\theta)) - T_n(x + G(\theta)) \\ \text{s.t.} \quad & x + G(\theta) \in [0, 1]^d, \quad \|G(\theta)\| < \epsilon, \quad q < q_{\max} \end{aligned} \quad (1)$$

For the image classification dataset considered we normalize the values of the pixels to  $[0, 1]$ . The components of  $G(\theta)$  and  $x + G(\theta)$  are clipped to  $[-\epsilon, \epsilon]$  and  $[0, 1]$  respectively to satisfy these constraints. For top  $n$  error, it is sufficient to have our objective function less than 0. Thus, the stopping condition for our algorithm is  $F_{\tau(x)}(x + G(\theta)) - T_n(x + G(\theta)) < 0$ .<sup>7</sup>

### 4.3 Bayesian Optimization

Bayesian optimization is a sequential model-based optimization algorithm primarily used to find optimal parameters  $\theta$  for black-box objective functions using a minimal number of queries [39, 63]. This technique has proven to be effective in solving various problems such as hyperparameter tuning, reinforcement learning, and combinatorial optimization [60].

Consider a set of functions parametrized by  $\theta$ . Let  $\mathcal{D}$  denote the observed data. We treat  $\theta$  as a latent variable with a prior distribution  $p(\theta)$ , this contains our prior beliefs on the values of  $\theta$ . Given the observations  $\mathcal{D}$  and a likelihood  $p(\mathcal{D} | \theta)$  we can compute the posterior  $p(\theta | \mathcal{D})$  using Bayes’ rule.

$$p(\theta | \mathcal{D}) = \frac{p(\mathcal{D} | \theta)p(\theta)}{p(\mathcal{D})}$$

<sup>6</sup>Where we can consider different type of norms.

<sup>7</sup>Similar to [10] more restrictive conditions can also be considered to produce adversarial examples with a higher level of confidence.

The posterior distribution is our updated belief on  $\theta$  given the observed data  $\mathcal{D}$  [56, 60]. In Bayesian optimization we use this model to update our assumptions on the parameters as we gather more observations from each query, with the goal of maximizing an objective function  $g$ . This algorithm is query efficient as it uses the information provided by past queries while also considering the uncertainty of the model.

Bayesian optimization consists of two components, first a probabilistic surrogate model, typically a Gaussian Process (GP), and, second, an acquisition function that guides its queries. GP regression is used to update the beliefs on the parameters with respect to the objective function after each query, and the acquisition function is used to select the next “best” input to query the target classifier. The algorithm stops once the best objective function value ceases to improve significantly or when it reaches its query budget [60].

**Gaussian Processes.** The first component in Bayesian optimization is a probabilistic surrogate model for our objective function. A GP is the generalization of Gaussian distributions to a distribution over functions and is typically used as the surrogate model for Bayesian optimization [56]. We use GPs as they induce a posterior distribution over the objective function that is analytically tractable. This allows us to update our beliefs of what the objective function looks like after each iteration [63].

A Gaussian Process  $\mathcal{GP}(m, k)$  is fully described by a prior mean function  $m : \mathcal{X} \rightarrow \mathbb{R}$  and positive-definite kernel or covariance function  $k : \mathcal{X} \times \mathcal{X} \rightarrow \mathbb{R}$ . We describe GP regression to understand how our GP is updated given more observations. Let  $\mathbf{X} = \mathbf{x}_{1:n}$  be a collection of  $n$  points and define variables  $f_i = f(\mathbf{x}_i)$  and  $\mathbf{y}_{1:n}$  to be unknown function values and noisy observations respectively. We assume that  $\mathbf{f} = f_{1:n}$  are jointly Gaussian and  $\mathbf{y} = y_{1:n}$  follow a normal distribution given  $\mathbf{f}$ . The following expressions give the GP prior and Gaussian likelihood respectively

$$\begin{aligned} p(f | \mathbf{X}) &= \mathcal{N}(m(\mathbf{X}), \mathbf{K}) \\ p(y | f, \mathbf{X}) &= \mathcal{N}(f(\mathbf{X}), \sigma^2 \mathbf{I}) \end{aligned}$$

where  $\mathcal{N}$  denotes a normal distribution. Elements of the mean and covariance matrix are given by  $m_i = m(\mathbf{x}_i)$  and  $K_{i,j} = k(\mathbf{x}_i, \mathbf{x}_j)$ . Given observations  $\{\mathbf{X}, \mathbf{y}\}$  and an arbitrary point  $\mathbf{x}$ , the updated posterior mean and covariance on the  $n$ -th query are given by

$$\begin{aligned} m_n(\mathbf{x}) &= m(\mathbf{x}) - (\mathbf{K} + \sigma^2 \mathbf{I})^{-1} (\mathbf{y} - m(\mathbf{X})) \\ k_n(\mathbf{x}, \mathbf{x}) &= k(\mathbf{x}, \mathbf{x}) - k(\mathbf{x}, \mathbf{X})(\mathbf{K} + \sigma^2 \mathbf{I})^{-1} k(\mathbf{X}, \mathbf{x}). \end{aligned}$$

We take the mean function to be zero  $m \equiv 0$  to simplify evaluation and since no prior knowledge can be incorporated into the mean function [60] as is the case for a black-box setting. The ability of GPs to model a rich distribution of functions rests on its kernel function which controls important properties of the function distribution such as differentiability, periodicity, and amplitude [56, 60]. Any prior knowledge of the target function is encoded in the kernel’s hyperparameters. In a restrictive black-box setting, we adopt a more general kernel function [63]. For our experiments we follow Snoek et al. [63] in choosing the Matérn 5/2 kernel

$$k_{5/2}(\mathbf{x}, \mathbf{x}') = \left( 1 + \frac{\sqrt{5}r}{l} + \frac{5r^2}{3l^2} \right) \exp\left(-\frac{\sqrt{5}r}{l}\right)$$

where  $r = \|\mathbf{x} - \mathbf{x}'\|$  and  $l$  is the length-scale parameter. This results in twice-differentiable functions, an assumption that corresponds to those made in popular black-box optimization algorithms like quasi-Newton methods [63].

**Acquisition Functions.** The second component in Bayesian optimization is an acquisition function that describes how optimal a query is. Intuitively, the acquisition function evaluates the utility of candidate points for the next evaluation, and it is normally defined so that high acquisition corresponds to potentially optimal values of the objective function [7].

We aim to maximize an objective function  $g$  and choose a general purpose acquisition function considering the black-box scenario. The two most popular choices are the *Expected Improvement* (EI) and Gaussian Process *Upper Confidence Bound* (UCB) [60]. First define  $\mu(\mathbf{x})$  and  $\sigma^2(\mathbf{x})$  as the predictive mean and variance of  $g(\mathbf{x})$  respectively. Let  $\gamma(\mathbf{x}) = \frac{g(\mathbf{x}_{\text{best}}) - \mu(\mathbf{x})}{\sigma(\mathbf{x})}$ . The acquisition functions are given by

$$\begin{aligned} \alpha_{\text{EI}}(\mathbf{x}) &= \sigma(\mathbf{x}) \gamma(\mathbf{x}) \Phi(\gamma(\mathbf{x})) + \mathcal{N}(\gamma(\mathbf{x}) | 0, 1) \\ \alpha_{\text{UCB}}(\mathbf{x}) &= \mu(\mathbf{x}) + \kappa \sigma(\mathbf{x}), \quad \kappa > 0 \end{aligned}$$

where  $\Phi$  is the normal cumulative distribution function.

EI and UCB have both been shown to be effective and data-efficient in real black-box optimization problems [63]. However, most studies have found that EI converges near-optimally, requires no tuning of its own parameters, and is better-behaved than UCB in the general case [7, 60, 63]. This makes EI the best candidate for our acquisition function.

#### 4.4 Parameters

In this section, we discuss how the parameters ( $\theta$ ), boundaries ( $\epsilon, q_{\text{max}}$ ), and evaluation metrics are chosen, selected, and used.

**Parameter Boundaries.** There are no formal metrics or heuristics we can follow a priori in a black-box setting to choose appropriate parameter boundaries. We visually inspect the generated patterns from a grid search of the parameters to identify ranges where the image has visually noticeable edges or curves, rather than entirely smooth or very noisy images. Note these parameter are dependent on the image dimensions, for this experiment it’s the input dimensions of our models: 299 by 299 by 3. For  $\theta_{\text{LGrad}} = \{v_a, v_b, \omega, v_{\text{sine}}\}$  we use:  $v_a, v_b \in [\frac{1}{20}, \frac{1}{160}]$ ,  $\omega \in \{1, 2, 3, 4\}$ , and  $v_{\text{sine}} \in [6, 32]$ . For  $\theta_{\text{SConv}} = \{N, \alpha, v, \omega, v_{\text{sine}}\}$  we use:  $N \in \{32, 64, 96\}$ ,  $\alpha, v \in [0.005, 0.5]$ ,  $\omega \in [0, \pi/2]$ , and  $v_{\text{sine}} \in [4, 26]$ .

**Parameter Selection.** We search over the parameter space randomly and with Bayesian optimization. For the former, we *randomly* draw parameters  $\theta$  for the noise function. This serves as a baseline performance and corresponds to a non-adaptive attack where the adversary indiscriminately injects noise. More queries leads to a higher likelihood of discovering parameters that cause top  $n$  error. With *Bayesian optimization*, we choose the parameters using a Gaussian Process, Matérn 5/2 kernel, and the expected improvement (EI) acquisition function as outlined in Sect. 4.3 for general black-box optimization [60].

Due to restrictions on the number of queries, exhaustive hyperparameter search methods such as grid search and gradient-based

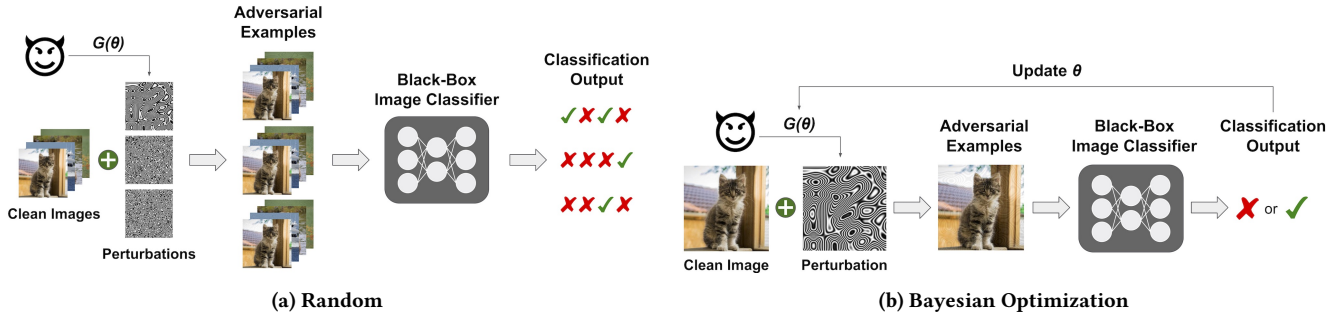


**Figure 3: A high-level illustration of procedural noise attacks with our parameter selection methods. Green checks and red crosses are correct and incorrect classification outputs respectively. The adversary generates perturbations  $G(\theta)$  with parameters  $\theta$ . For random, the adversary indiscriminately injects clean images with various perturbations generated by different randomly chosen  $\theta$ . For Bayesian optimization, the attack queries with one  $\theta$  at a time for a given image, and if it unsuccessful in evading, the parameter  $\theta$  for their next query is updated using output probabilities  $F(x)$ .**

optimization are not viable. We use Bayesian optimization as our only query-efficient parameter selection strategy.

**Error Metrics.** Given a classifier and input  $x$ , an adversarial example  $x'$  is “successful” when it achieves top  $n$  error within the problem constraints. Recall top  $n$  error is when the true label is not within the top  $n$  probability scores. Top  $n$  error for a classifier is the proportion of inputs that the attack is successful against. Attack performance is measured using top 1 and top 5 error ( $n = 1, 5$ ).

**Maximum Queries.** There are no formal guarantees that there exists a set of parameters that generate successful adversarial perturbations, so we set a maximum budget  $q_{\max}$  to keep the number of queries within a reasonable range. For Bayesian optimization, exact inference in Gaussian Process regression is  $O(q^3)$  where  $q$  is the number of observations or queries. This cost is due to the inversion of the covariance matrix when updating the posterior. Because of this restriction, we set  $q_{\max} = 100$ . This upper bound proved to be sufficient as our experiments show the attacker’s performance begins to plateau as  $q$  approaches  $q_{\max}$ .

**Distance Metric.** The distance metric is a useful heuristic to quantify similarity between images. The usual metric is the  $\ell_p$  norm since images are visually similar if their difference  $r$  satisfies  $\|r\| < \epsilon$  for a sufficiently small  $\epsilon$ . For the  $\ell_\infty$  norm, the largest possible difference between any coordinate is limited by  $\epsilon$ , so we have  $\|r_i\| < \epsilon$  for all points  $i$ . Because of its pixel-wise construction, our noise function is best measured with the  $\ell_\infty$  norm. For the ImageNet dataset, we follow the  $\ell_\infty$  norm upper bounds of  $\epsilon \leq \frac{16}{256}$  as in previous studies [30, 69].

## 5 EXPERIMENT SETUP

In this section we detail the dataset, models, attacks, and metrics used for our black-box procedural noise attack.

### 5.1 Dataset & Models

The ImageNet dataset tested on is from the image classification task of the ILSVRC2012 validation set [57]. It is a widely used object recognition benchmark with images taken from various search engines and manually labelled to 1,000 distinct object categories where each image is assigned one ground truth label.

We use pre-trained ImageNet models that have the *Inception v3* [66] and *Inception ResNet v2* [65] models abbreviated as **v3** and **IRv2** respectively. These models achieve state-of-the-art performance with top 5 error of 6.3% and 4.7% respectively. These networks take images with dimensions  $299 \times 299 \times 3$  as input. Note our chosen models are generally more robust when compared to other architectures such as ResNet50 [18] or VGG [62], which achieve top 5 error of up to 7.9% and 10.0% respectively.

We also take adversarially trained versions of the more robust Inception ResNet v2: Tramer et al. [69] adversarially train the Inception ResNet v2 following the methodology of [30], this network will be referred to as **IRv2<sub>adv</sub>**. Tramer et al. extend this to a model with ensemble adversarial training, which we refer to as **IRv2<sub>adv-ens</sub>**. These have the same architecture, but different weights when compared to IRv2. For complete details of the adversarial and ensemble adversarial training process, we refer the reader to [30] and [69]. Taking models from [69] allows us to test our attack against the most robust models and better compare our attacks with other attacks on these same ImageNet classifiers.

We evaluate our procedural noise attacks on 5,000 random images from the validation set, a budget of at most  $q_{\max} = 100$  queries per image, and an  $\ell_\infty$  norm constraint of  $\epsilon \leq \frac{16}{256}$ .

### 5.2 Procedural Noise Attacks

We use our generating function to create adversarial perturbations  $G(\theta)$  a given parameter setting. For each image  $x$  we query the classifier  $x + G(\theta)$  clipped to the maximum perturbation  $\epsilon = \frac{16}{256}$  and image domain  $[0, 1]^d$ . For each query we update  $\theta$  either randomly or using Bayesian optimization.

**Random.** We randomly generate 100 distinct parameter settings  $\theta$  within the parameter boundaries described in Sect. 4.4 and iterate over these when querying the classifier for each image. This is how each parameter setting counts as one query for an image.

**Bayesian Optimization.** We attack images one at a time with the goal of achieving top 5 error. To initialize Bayesian optimization we first randomly choose 10 different parameter settings to query the classifier. Afterwards, we update our choice of parameters using Bayesian optimization and objective function (1) with  $n = 5$ . The

**Table 1: Error (in %) for procedural noise attacks on ImageNet for 5,000 random validation set samples with  $\epsilon = 16/256$  and  $q_{\max} = 100$  per sample. Strongest attack on each classifier is highlighted.**

Classifier	Top 1 Error					Top 5 Error				
	Original	LGrad-R	LGrad-B	SConv-R	SConv-B	Original	LGrad-R	LGrad-B	SConv-R	SConv-B
v3	22.7	79.3	<b>80.0</b>	68.1	51.3	6.3	55.3	<b>58.2</b>	40.4	22.6
IRv2	20.1	69.5	<b>71.2</b>	57.6	42.5	4.5	44.3	<b>46.3</b>	31.3	17.3
IRv2 <sub>adv</sub>	19.7	64.9	<b>66.7</b>	51.8	38.4	4.6	38.9	<b>41.0</b>	24.0	14.8
IRv2 <sub>adv-ens</sub>	20.2	61.1	<b>62.7</b>	45.0	34.5	5.3	35.4	<b>37.4</b>	18.8	12.4

stopping condition is met when the adversarial example causes top 5 error or when the number of queries reaches  $q_{\max} = 100$ .

### 5.3 Evaluation Methodology

To measure the performance of our attack, we use the metrics described in Sect. 2: general score, transferability, universality, and query efficiency. For each of these metrics, we compare our procedural noise attack with comparable existing attacks, noting that our attack assumes less adversary knowledge and capabilities in all cases. When reporting results, we refer to our procedural noise attacks with **LGrad** for Lattice Gradient Noise and **SConv** for Sparse Convolution Noise, and use the suffixes **-R** for random and **-B** for Bayesian optimization.

## 6 ATTACK PERFORMANCE

Despite a good performance on the original images, our results (Table 1) show the classifiers having a significantly high error on our procedural noise adversarial examples. The lattice gradient noise (LGrad) greatly degrades the performance of all classifiers for both top 1 and 5 error. Top 5 performance is more difficult to degrade than top 1 since it is harder to remove as the former considers more labels. Despite this, a top 5 error of at least 40% is attained for all classifiers with our LGrad attack. This shows a significant vulnerability to such perturbations.

Classifiers that generalize better are more robust to perturbations [30], so the result between classifiers is expected. The Inception ResNet v2 architecture has shown to achieve better performance than the Inception v3 architecture [65]. Across the Inception ResNet v2 networks, the adversarial and ensemble training marginally improve their performance against our procedural noise attacks, but it is not a robust defence.

**Lattice Gradient vs Sparse Convolution.** Both procedural noise attacks significantly impact the accuracy of the target models. However, LGrad outperforms SConv and the latter achieves even worse performance with Bayesian optimization. In theory, Bayesian optimization would be able to utilize the limited queries to get better performance than random sampling. However Bayesian optimization can be limited when it has less queries and more parameters to search over, which is the case with SConv. The sparse convolution noise  $G_{\text{SConv}}$  may also have introduced non-stationarity in the objective function with respect to its parameters. This non-stationary property is not captured by a Matérn kernel and would cause poor predictions in the optimization algorithm. Exploring other Bayesian optimization settings and assumptions

**Table 2: Comparison between our procedural noise attack and fast gradient attacks by Tramer et al. [69]. Error (in %) on ImageNet with  $\epsilon = 16/256$ . Strongest attack is highlighted.**

Classifier	Top 1 Error			Top 5 Error		
	LGrad	FG-W	FG-B	LGrad	FG-W	FG-B
v3	<b>80.0</b>	69.6	51.2	<b>58.2</b>	42.7	24.5
IRv2	<b>71.2</b>	50.7	44.4	<b>46.3</b>	24.0	17.8
IRv2 <sub>adv</sub>	<b>66.7</b>	21.4	34.5	<b>41.0</b>	5.8	11.7
IRv2 <sub>adv-ens</sub>	<b>62.7</b>	26.0	27.0	<b>37.4</b>	7.6	7.9

warrants further study. From here on, we focus on the results of the performing LGrad attack.

### 6.1 Comparison with Fast Attacks

Our procedural noise attack is computationally inexpensive and fast to generate, which leads us to compare our attack against popular white-box algorithms that efficiently generate adversarial examples.

The three algorithms we compare to are Fast Gradient Sign Method (FGSM), Single-Step Least-Likely Class Method (Step-LL), and Iterative Attack (Iter-LL) [16, 29, 69]. These methods use gradient based optimization to generate adversarial examples with a bounded  $\ell_{\infty}$  norm. FGSM and Step-LL are “single-step”-requiring only one gradient computation, and Iter-LL requires only a bounded number of gradient computations [29, 69]. These inherently make a trade-off favoring computation speed over effectiveness when compared to other white-box algorithms.

We refer to these three algorithms collectively as fast gradient attacks (FG) and distinguish between white-box (FG-W) and partial black-box (FG-B) versions. In practical settings, FG attacks require white-box adversaries or, in the case of transfer attacks, partial black-box adversaries. Though more iterations would yield to higher attack success on the white-box model, it is not always favorable in transfer attacks as more iterations make the adversarial example overfit to the white-box model resulting in poor transferability [73].

In Table 2, we compare our procedural noise attack with attacks from Tramer et al. on the same classifiers and perturbation constraint  $\epsilon = \frac{16}{256}$  [69]. FG-W here refers to a white-box Step-LL attack while FG-B refers to the strongest transfer attack crafted with Step-LL, FGSM, or I-FGSM.

As shown in Table 2, our LGrad attack greatly outperforms FG-B and edges over the FG-W attack. Though the random samples for

both experiments may differ, they are drawn from similar distributions. Hence, the large disparity in performance between LGrad and FG-B attacks can not be explained away by the test samples. The drop in performance of FG-B and FG-W against IRv2<sub>adv</sub> and IRv2<sub>adv-ens</sub> is reasonable as the adversarial training was designed specifically to defend against these attacks, but adversarial training still does not significantly diminish the effect of the LGrad attack.

Our LGrad attack achieves comparable performance to FG-W and almost double that of FG-B despite using a significantly weaker restricted black-box adversary. We hypothesize that our procedural noise attack takes advantage of inherent weaknesses in the learning algorithms and their interpretations of patterns within images, allowing it to fool the classifier in a few queries. In contrast, existing methods that use gradient-based optimization do not find adversarial examples within a few gradient computations due to the high dimensionality of the input space. This also explains why the FG attacks falter on top 5 error as they require more iterations.

## 6.2 Universality & Transferability

The transferability and universality of adversarial examples are strong indicators of an attack’s generalizability. It is surprising that random parameter selection achieves very good results against the classifiers. This indicates a systemic fragility of these neural networks to our procedural noise attacks. In our random parameter attacks, LGrad-R and SConv-R, we test the same 100 adversarial perturbations across all images for all classifiers. For this analysis we focus on the stronger LGrad procedural noise.

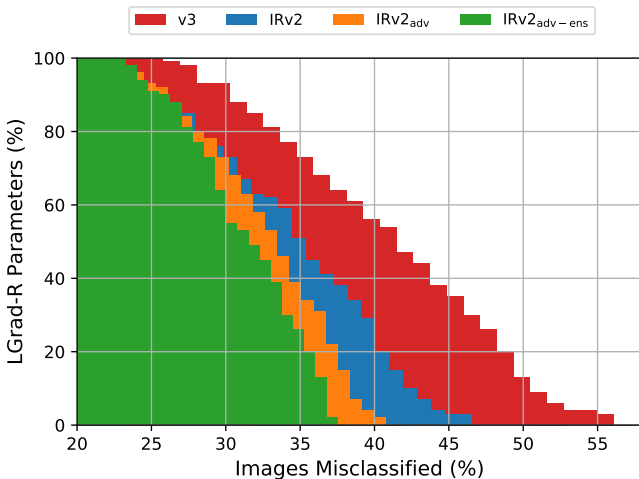


Figure 4: Universal top 1 error of LGrad-R parameters.

Each LGrad parameter setting corresponds to a noise pattern and the universal top 1 error of a parameter setting is the fraction of the 5,000 random samples that its perturbation causes top 1 error on. For example, Fig. 4 shows that 20% (y-axis) of the randomly chosen LGrad parameters achieve a universal top 1 error of at least 35% on IRv2<sub>adv-ens</sub>, 37% on IRv2<sub>adv</sub>, 40% on IRv2, and 48% on v3. The robustness of the IRv2 architecture over v3 becomes apparent here, and both adversarially trained models perform slightly better than the original IRv2. The universality of *random* parameters is

Table 3: Universal top 1 error (in %) of top LGrad-R perturbations. Strongest parameters per classifier are highlighted.

$\theta_{\text{LGrad}} = \{v_a, v_b, \omega, v_{\text{sine}}\}$	Classifier			
	v3	IRv2	IRv2 <sub>adv</sub>	IRv2 <sub>adv-ens</sub>
#1 {0.0142, 0.0132, 1, 30.01}	54.5	45.6	<b>42.7</b>	<b>39.9</b>
#2 {0.0157, 0.0132, 3, 29.60}	58.1	48.3	41.9	39.6
#3 {0.0217, 0.0178, 3, 23.49}	58.0	<b>48.6</b>	40.7	37.5
#4 {0.0356, 0.0449, 2, 15.83}	<b>58.2</b>	48.4	39.6	34.5
#5 {0.0124, 0.0218, 1, 31.47}	57.0	45.9	41.4	39.2

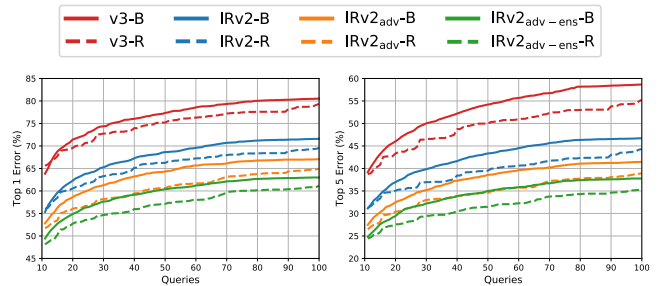


Figure 5: Error versus queries for LGrad attacks with (left) top 1 error and (right) top 5 error.

a concern as it degrades the classifiers’ performance on a large fraction of these images.

**Cross-Model Universality.** In the interest of finding the “best” universal adversarial perturbation (UAP), we take the LGrad-R parameter values that achieve the highest error and measure how well they perform across all the classifiers. The rightmost tail in Fig. 4 corresponds to our UAP parameters, and these values align with Table 3. We find that the parameters that are universal on one tend to generalize across the models despite differences in architectures and weights. Each of these individual UAP parameters achieve upwards of 35% top 1 error across all classifiers.

This shows that our procedural noise adversarial examples generalize across images and models, making it a very potent adversary. To our knowledge, this is the first model-agnostic (black-box) generation of universal adversarial perturbations.

## 6.3 Query Efficiency

In restrictive black-box settings, it is practical to limit queries to avoid detection. We measure the attack performance of our LGrad procedural noise attack as a function of the number of queries performed. In Fig. 5 we suffix each classifier with the parameter selection method ‘-B’ or ‘-R’ and begin plotting from the 11th query since our Bayesian optimization uses 10 queries for initialization.

**Bayesian Optimization vs Random.** We explained earlier why SConv-B performs worse than SConv-R due to restrictive assumptions and a larger search space. For LGrad, Bayesian optimization outperforms random queries, but the latter is surprisingly close due to the universality of the LGrad-R procedural noise.

In Fig. 5, Bayesian optimization consistently performs better than random parameter selection past 15 queries for both top 1 and top 5

**Table 4: Number of queries for LGrad-B to equal or surpass the performance of 100 queries from LGrad-R.**

Classifier	Top 1 Error	Top 5 Error
v3	59	46
IRv2	49	48
IRv2 <sub>adv</sub>	44	43
IRv2 <sub>adv-ens</sub>	49	43

**Table 5: Comparison of LGrad-B procedural noise attack with bandit attack by Ilyas et al. on Inception v3 [23].**

	Bandit	LGrad-B
Top 1 Error (%)	92.9	75.5
Avg. # Queries	1,180	38
% of Bandit Score	100.0	81.3
% of Bandit Avg. Queries	100.0	3.2

error. The improvement in performance that Bayesian optimization gives over random becomes more apparent for top 5 error. This may be because moving the true label out of the top 5 predictions is a more challenging task that requires a guided approach that makes use of past queries.

In Table 4, we measure the minimum number of queries Bayesian optimization needed to match the performance of the 100 random queries. Our results show that Bayesian optimization only needs 43-59% of queries to attain similar performance to random, saving 52.4% queries on average.

**Comparison with Bandits.** A strong restrictive black-box attack is a bandit optimization framework by Ilyas et al. where they achieve 92.9% top 1 error averaging a thousand queries per image [23]. Du et al. was also considered, but due to the large variance with their average number of queries depending on their “region size” parameter [13], we choose to compare directly with Ilyas et al.’s method instead.

Ilyas et al. formalize their objective to a gradient estimation problem and use bandit optimization to solve it in a query-constrained black-box scenario. Bandit optimization is a tool used in online convex optimization where a limited set of resources (queries) is allocated between competing decisions to maximize an expected gain [23]. Their gradient estimation substitutes for the gradient-based optimization that has shown to be effective in existing white-box adversarial attacks.

We replicate their experiment with our LGrad-B procedural noise attack, using  $\epsilon = 0.05$  and 2,000 *correctly classified* random validation samples on Inception v3. As in past experiments, we also set our query budget to  $q_{\max} = 100$ , which is significantly less than the 10,000 limit in the bandits framework. Table 5 shows that our attack achieves up to 81.3% of the bandit’s score with 3.2% of the average number of queries. Though our attack does not reach the same score, it is  $81.3 / 3.2 = 25.4$  times more query efficient. Comparing it with an attack that achieves 100% at 1,000 queries on average like in the best case of [13], the improvement in efficiency is 23.6 fold.

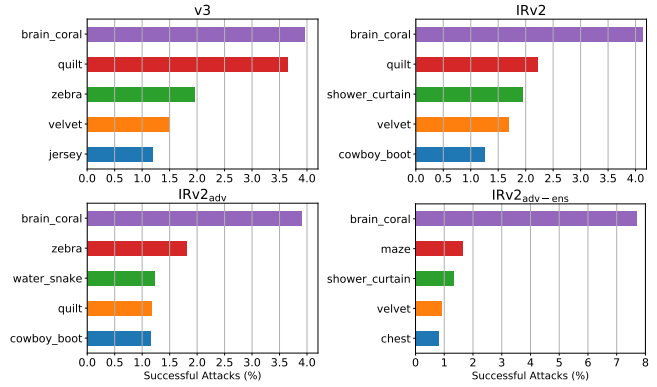


**Figure 6: Class label distribution of successful LGrad-R adversarial examples.**

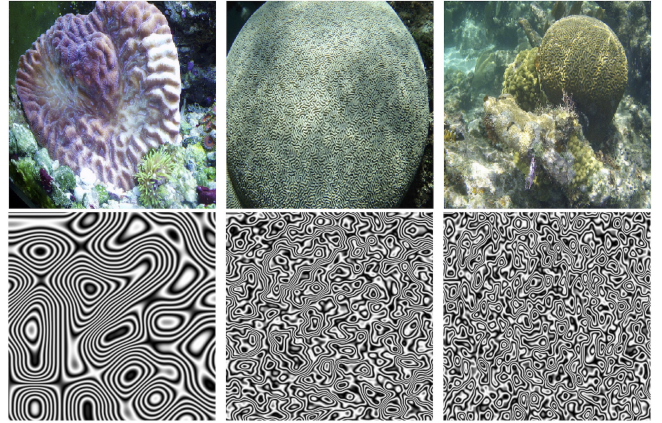


**Figure 7: (top) “brain\_coral” examples from ImageNet dataset. (bottom) visualization of universal adversarial perturbations:  $\theta_{\text{LGrad}}$  #1, #3, and #4 from Table 3.**

## 6.4 Label Analysis

Our procedural noise attack is indiscriminate with respect to target labels, so it is useful to understand which labels our adversarial examples are most frequently classified under. We focus on LGrad-R as it outperforms SConv and the 100 random parameters were tested for each validation image on each classifier. Bayesian optimization results are not representative of the LGrad noise as it generated only one adversarial example per image. Figure 6 shows the 5 most prominent class labels as a percentage of all *successful* top 1 attacks for LGrad-R. We can see differences across architectures (v3, IRv2) and across training methods on the same IRv2 architecture.

In Fig. 6, we observe that IRv2<sub>adv-ens</sub> is an outlier among the classifiers as “brain\_coral” corresponds to a disproportionately larger percentage of adversarial examples. “brain\_coral” corresponds to 8% of adversarial examples in IRv2<sub>adv-ens</sub> compared to less than 2% of other class labels for that model. When compared to the remaining three classifiers, “brain\_coral” is around 4% with other labels like “quilt” or “zebra” not far behind. We hypothesize that adversarial training like in IRv2<sub>adv</sub> made non-“brain\_coral” labels less likely

than in IRv2, while ensemble adversarial training takes it even further. These imply that our LGrad procedural noise strongly activates the “brain\_coral” class, as the most robust model IRv2<sub>adv-ens</sub> still gets tricked into classifying it as such.

In Fig. 7 we see visual similarities between “brain\_coral” and our LGrad perturbations. Despite this, there are generally two types of objects whose labels came out on top in Fig. 6: (a) those with high-frequency patterns such as “brain\_coral”, “zebra”, and “maze”, and (b) items made of cloths or fabrics such as “shower curtain”, “velvet”, and “quilt”. The latter type of items usually have printed patterns or they tend to fold or crease—giving a wavy appearance. These class labels are visually similar to our procedural noise, which may explain why our generated adversarial examples are classified towards these labels.

The textures these class labels contain are similar to basic edges, textures, and patterns that are learned by the initial layers of the neural network as visualized by [45]. Deeper layers of network usually learn more complex features such as body parts or entire objects [45]. Deep neural networks trained on natural images, such as ImageNet, learn basic features in the first layers that are similar in appearance to edge filters and color blobs [45, 72]. This phenomenon is used in transfer learning where the first few layers and weights from a model trained in one task are used to initialize the training of another model in a similar task [46, 72]. However, this similarity between initial layers can also explain why vulnerabilities generalize across inputs and models. The basic features that the networks learn resemble basic patterns that are visually similar to procedural noise. This may imply that our procedural noise attack exploits these first few layers as they correspond to the basic textures that the networks learn.

## 7 DISCUSSION

The deep neural networks (DNNs) we test are surprisingly fragile to procedural noise, and it is most apparent with the cross-model universality of a few *randomly* generated adversarial perturbations. Procedural noise is typically used for generating natural images in computer graphics, so it may replicate features learned by the DNNs. Thus, the added noise affects the final decision of the model. Because it is easy to compute and fast to generate, procedural noise can be used as a benchmark to test the robustness of image classification systems to additive noise.

### 7.1 Defences

Making neural networks robust to adversarial examples is not a straightforward task. A robust defence needs to not only defend against existing attacks but also possible future attacks. Athalye et al. and Carlini et al. demonstrate the deficiencies of existing defences by breaking defensive distillation [10], gradient obfuscation [1], and adversarial example detection [9].

Among the remaining defences, adversarial training has shown to be more robust than others [1]. Kurakin et al. implement adversarial training on ImageNet and showed that it confers robustness to single-step gradient attacks [30]. Madry et al. used Projected Gradient Descent (PGD) and demonstrated that adversarial training with examples from their PGD attack grants resilience against other first-order gradient attacks [35]. Tramer et al. then propose

ensemble adversarial training to augment the training data with adversarial examples from other models, and it has shown reasonable success against black-box attacks on ImageNet [69]. The idea of ensemble adversarial training is to decouple the generation of adversarial examples from the model, but these adversarial examples were generated with fast gradient attacks.

A notable flaw with existing evaluations is the reliance on attacks that make use of gradient-based optimization (gradient descent). Adversarial training is still vulnerable to new attacks, like procedural noise, that do not use gradient-based optimization. In Table 1 we show that adversarial training IRv2<sub>adv</sub> and ensemble adversarial training IRv2<sub>adv-ens</sub> conferred improved robustness when compared to the original IRv2. However, it did not significantly diminish the impact of our procedural noise attacks.

Adversarial training with our procedural noise may not be sufficient either as it is difficult to account for all possible noise variations. To illustrate the variety of procedural noise, our noise generating function  $G_{\text{LGrad}}$  uses only four parameters with a basic lattice gradient noise algorithm and a greyscale colour map. Instead of Perlin noise, functions with more parameters such as Gabor noise could have been used, and beyond that there are still multiple types of noise under each of the three noise families (lattice gradient, explicit, and sparse convolution). For the colour map, instead of just the sine function, a wide variety of mathematical functions can be composed to form even more complex patterns. The colour map can also be expanded to affect the three colour channels (red, green, blue) in different ways.

The attacker can continually change their approach or perspective, making it difficult to defend against all attacks. So far, adversarial perturbations can be generated with: (a) gradient-based optimization, (b) spatial transformations such as rotation [14, 71], translation, scaling, warping, and (c) procedural noise functions. The latter two types of attacks have yet to be thoroughly explored, and there may be more undiscovered attacks.

In its current state, it becomes computationally intractable to train neural networks on all types of perturbations and we argue that adversarial training *on its own* is insufficient. This also applies for methods that are designed to detect or denoise specific adversarial perturbations. We hypothesize that the underlying problem lies with how and what the neural network learns, and this can be improved on by understanding their learned features and developing more robust learning algorithms.

### 7.2 Limitations

Due to the restrictive black-box setting, our procedural noise attack naturally has several limitations. We made numerous trade-offs, giving up attack complexity and performance in favour of speed, scalability, query-efficiency, and computational inexpensiveness. This was to show that our attacks are practical and easy to perform. However, given a more generous constraint on queries, other black-box attacks like the bandit optimization framework [23] or more exhaustive search methods like grid search may be preferred as Bayesian optimization scales poorly with the number of queries.

The selection of procedural noise functions and parameter boundaries was done based on heuristics of our observations on existing

adversarial perturbations. We relied on intuition and visual inspection to identify procedural noise functions and parameter boundaries that would have the appearance of curves and edges across the image. Because of this, there are no theoretical guarantees that the attack can succeed, i.e. given an image and set of constraints it’s difficult to determine if there exists a parameter setting  $\theta$  for our generating function  $G(\theta)$  that is capable of fooling the classifier.

For the experiment, we limited the attacks to 100 random parameter settings, which may have skewed the results in either way. Despite this, the results with Bayesian optimization show that the performance of the random attacks were feasible. Because the generation of procedural noise is specific to computer vision, it is also worth exploring its effectiveness in other computer vision tasks such as object detection, semantic segmentation, and facial recognition, to name a few.

### 7.3 Beyond Images

Adversarial machine learning research has predominantly been computer vision driven [9, 50] due to (a) the accessibility of labelled images, wide adoption of benchmark datasets, and (b) the intuitive nature of vision for humans. Humans are equipped with their own vision systems which makes it easier to quickly identify and verify adversarial examples as well as understand manipulations applied to images. As a result, research is more challenging for other applications such as malware detection and reinforcement learning because the notion of an adversarial perturbation is not as intuitive or easy to evaluate and verify in these domains.

Exploring the vulnerabilities of deep learning to high-frequency low-intensity noise patterns in sensory data applications such as vision and audio is a natural next step. To expand our procedural noise attack framework to other applications, it is worth identifying patterns in adversarial examples for domains like speech recognition [8, 11] and deep reinforcement learning [22, 33] to find analogues of procedural noise. Finding intuitive adversarial examples may be easier against reinforcement learning in particular since computer vision is involved in some of its use cases, especially where learning agents take in visual data as input [22, 33, 38].

## 8 CONCLUSION

We have shown that existing state-of-the-art neural network image classifiers have systemic vulnerabilities to adversarial examples that are based on procedural noise functions. Our evaluation was conducted on a large-image dataset. More notably, our procedural noise perturbations generalize as universal adversarial perturbations (UAP), with the more powerful perturbations able to degrade performance across different classifiers. To our knowledge, this is the first model-agnostic generation of UAPs. Our black-box attack achieves comparable performance to existing white-box algorithms for generating fast adversarial examples and twice that of black-box transfer attacks, outperforming stronger adversaries for fast adversarial examples. In restrictive black-box settings the attack can achieve 75.5% success with 38 queries on average, which is a 25 fold improvement on existing restrictive black-box attacks on ImageNet models.

Our results have notable implications. The random version of our attack introduces the possibility for large-scale denial of service on

DNN-based image classification services, and the use of Bayesian optimization makes black-box attacks significantly more query efficient. From our observations, we postulate that this systemic vulnerability is related to the basic features that DNNs learn in their initial layers. We have shown the difficulty of defending against such novel approaches, and in particular that ensemble adversarial training was unable to fully negate our attack. The adversarial machine learning literature has so far mostly focused on gradient-based optimization techniques. Although these are effective, other attack algorithms should be explored to have a more complete characterization of vulnerabilities present in neural networks.

Our work prompts the need for further research of more intuitive and novel attack frameworks that can find analogues of procedural noise in other computer vision applications, e.g. object detection, semantic segmentation, as well as other machine learning application domains such as audio processing and reinforcement learning. As a basic denoising technique for images, we can suggest low pass filters or total variation denoising because adversarial examples tend to be high-frequency noise patterns, but this may not cover all possible perturbations. We hope future work will explore in more depth the nature of universal and transferable adversarial examples, as these vulnerabilities generalize across models and seem to be linked with why our procedural noise attack is effective.

## REFERENCES

- [1] Anish Athalye, Nicholas Carlini, and David Wagner. 2018. Obfuscated Gradients Give a False Sense of Security: Circumventing Defenses to Adversarial Examples. *arXiv preprint arXiv:1802.00420* (2018).
- [2] Marco Barreno, Blaine Nelson, Russell Sears, Anthony D Joseph, and J Doug Tygar. 2006. Can Machine Learning Be Secure?. In *Symposium on Information, Computer and Communications Security*. 16–25.
- [3] Arjun Nitin Bhagoji, Warren He, Bo Li, and Dawn Song. 2018. Black-box Attacks on Deep Neural Networks via Gradient Estimation. (2018).
- [4] Battista Biggio, Igino Corona, Davide Maiorca, Blaine Nelson, Nedim Šrđić, Pavel Laskov, Giorgio Giacinto, and Fabio Roli. 2013. Evasion Attacks against Machine Learning at Test Time. In *Joint European Conference on Machine Learning and Knowledge Discovery in Databases*. 387–402.
- [5] Battista Biggio, Blaine Nelson, and Pavel Laskov. 2012. Poisoning Attacks against Support Vector Machines. In *International Conference on International Conference on Machine Learning*. 1467–1474.
- [6] Mariusz Bojarski, Davide Del Testa, Daniel Dworakowski, Bernhard Firner, Beat Flepp, Praseon Goyal, Lawrence D Jackel, Mathew Monfort, Urs Muller, Jiakai Zhang, et al. 2016. End to end learning for self-driving cars. *arXiv preprint arXiv:1604.07316* (2016).
- [7] Eric Brochu, Vlad M Cora, and Nando De Freitas. 2010. A Tutorial on Bayesian Optimization of Expensive Cost Functions, with Application to Active User Modeling and Hierarchical Reinforcement Learning. *arXiv preprint arXiv:1012.2599* (2010).
- [8] Nicholas Carlini, Pratyush Mishra, Tavish Vaidya, Yuankai Zhang, Micah Sherr, Clay Shields, David Wagner, and Wencho Zhou. 2016. Hidden Voice Commands.. In *USENIX Security Symposium*. 513–530.
- [9] Nicholas Carlini and David Wagner. 2017. Adversarial Examples are not Easily Detected: Bypassing Ten Detection Methods. In *Workshop on Artificial Intelligence and Security*. 3–14.
- [10] Nicholas Carlini and David Wagner. 2017. Towards Evaluating the Robustness of Neural Networks. In *Symposium on Security and Privacy*. 39–57.
- [11] Nicholas Carlini and David Wagner. 2018. Audio adversarial examples: Targeted attacks on speech-to-text. *arXiv preprint arXiv:1801.01944* (2018).
- [12] Pin-Yu Chen, Huan Zhang, Yash Sharma, Jinfeng Yi, and Cho-Jui Hsieh. 2017. Zoo: Zeroth Order Optimization Based Black-box Attacks to Deep Neural Networks without Training Substitute Models. In *Workshop on Artificial Intelligence and Security*. 15–26.
- [13] Yali Du, Meng Fang, Jinfeng Yi, Jun Cheng, and Dacheng Tao. 2018. Towards Query Efficient Black-box Attacks: An Input-free Perspective. In *Proceedings of the 11th ACM Workshop on Artificial Intelligence and Security*. ACM, 13–24.
- [14] Logan Engstrom, Dimitris Tsipras, Ludwig Schmidt, and Aleksander Madry. 2017. A Rotation and a Translation Suffix: Fooling CNNs with Simple Transformations. *arXiv preprint arXiv:1712.02779* (2017).

- [15] Jiashi Feng, Huan Xu, Shie Mannor, and Shuicheng Yan. 2014. Robust Logistic Regression and Classification. In *Advances in Neural Information Processing Systems*. 253–261.
- [16] Ian J Goodfellow, Jonathon Shlens, and Christian Szegedy. 2014. Explaining and Harnessing Adversarial Examples. *arXiv preprint arXiv:1412.6572* (2014).
- [17] Kathrin Grosse, Nicolas Papernot, Praveen Manoharan, Michael Backes, and Patrick McDaniel. 2016. Adversarial perturbations against deep neural networks for malware classification. *arXiv preprint arXiv:1606.04435* (2016).
- [18] Kaiming He, Xiangyu Zhang, Shaoqing Ren, and Jian Sun. 2016. Deep residual learning for image recognition. In *Proceedings of the IEEE conference on computer vision and pattern recognition*. 770–778.
- [19] Geoffrey Hinton, Li Deng, Dong Yu, George E Dahl, Abdel-rahman Mohamed, Navdeep Jaitly, Andrew Senior, Vincent Vanhoucke, Patrick Nguyen, Tara N Sainath, et al. 2012. Deep Neural Networks for Acoustic Modeling in Speech Recognition: The Shared Views of Four Research Groups. *IEEE Signal Processing Magazine* 29, 6 (2012), 82–97.
- [20] Elike Hodo, Xavier Bellekens, Andrew Hamilton, Pierre-Louis Dubouilh, Ephraim Iorkyase, Christos Tachtatzis, and Robert Atkinson. 2016. Threat analysis of IoT networks using artificial neural network intrusion detection system. In *Networks, Computers and Communications (ISNCC), 2016 International Symposium on*. IEEE, 1–6.
- [21] Ling Huang, Anthony D Joseph, Blaine Nelson, Benjamin IP Rubinstein, and JD Tygar. 2011. Adversarial machine learning. In *Workshop on Security and Artificial Intelligence*. 43–58.
- [22] Sandy Huang, Nicolas Papernot, Ian Goodfellow, Yan Duan, and Pieter Abbeel. 2017. Adversarial attacks on neural network policies. *arXiv preprint arXiv:1702.02284* (2017).
- [23] Andrew Ilyas, Logan Engstrom, and Aleksander Madry. 2018. Prior convictions: Black-box adversarial attacks with bandits and priors. *arXiv preprint arXiv:1807.07978* (2018).
- [24] Ahmad Javaid, Qamar Niyaz, Weiqing Sun, and Mansoor Alam. 2016. A deep learning approach for network intrusion detection system. In *Proceedings of the 9th EAI International Conference on Bio-inspired Information and Communications Technologies (formerly BIONETICS)*. ICST (Institute for Computer Sciences, Social-Informatics and ?), 21–26.
- [25] Min-Joo Kang and Je-Won Kang. 2016. Intrusion detection system using deep neural network for in-vehicle network security. *PLoS one* 11, 6 (2016), e0155781.
- [26] Marius Kloft and Pavel Laskov. 2012. Security Analysis of Online Centroid Anomaly Detection. *Journal of Machine Learning Research* 13 (2012), 3681–3724.
- [27] Pang Wei Koh and Percy Liang. 2017. Understanding Black-box Predictions via Influence Functions. In *International Conference on Machine Learning*. 1885–1894.
- [28] Alex Krizhevsky, Ilya Sutskever, and Geoffrey E Hinton. 2012. Imagenet Classification with Deep Convolutional Neural Networks. In *Advances in Neural Information Processing Systems*. 1097–1105.
- [29] Alexey Kurakin, Ian Goodfellow, and Samy Bengio. 2016. Adversarial Examples in the Physical World. *arXiv preprint arXiv:1607.02533* (2016).
- [30] Alexey Kurakin, Ian Goodfellow, and Samy Bengio. 2016. Adversarial Machine Learning at Scale. *arXiv preprint arXiv:1611.01236* (2016).
- [31] Ares Lagae, Sylvain Lefebvre, Rob Cook, Tony DeRose, George Drettakis, David S Ebert, John P Lewis, Ken Perlin, and Matthias Zwicker. 2010. A Survey of Procedural Noise Functions. In *Computer Graphics Forum*, Vol. 29. 2579–2600.
- [32] Ares Lagae, Sylvain Lefebvre, George Drettakis, and Philip Dutré. 2009. Procedural noise using sparse Gabor convolution. *ACM Transactions on Graphics (TOG)* 28, 3 (2009), 54.
- [33] Yen-Chen Lin, Zhang-Wei Hong, Yuan-Hong Liao, Meng-Li Shih, Ming-Yu Liu, and Min Sun. 2017. Tactics of adversarial attack on deep reinforcement learning agents. *arXiv preprint arXiv:1703.06748* (2017).
- [34] André Teixeira Lopes, Edilson de Aguiar, Alberto F De Souza, and Thiago Oliveira-Santos. 2017. Facial expression recognition with convolutional neural networks: coping with few data and the training sample order. *Pattern Recognition* 61 (2017), 610–628.
- [35] Aleksander Madry, Aleksandar Makelov, Ludwig Schmidt, Dimitris Tsipras, and Adrian Vladu. 2017. Towards Deep Learning Models Resistant to Adversarial Attacks. *arXiv preprint arXiv:1706.06083* (2017).
- [36] Patrick McDaniel, Nicolas Papernot, and Z Berkay Celik. 2016. Machine Learning in Adversarial Settings. *IEEE Security & Privacy* 14, 3 (2016), 68–72.
- [37] Shike Mei and Xiaojin Zhu. 2015. Using Machine Teaching to Identify Optimal Training-Set Attacks on Machine Learners. In *AAAI*. 2871–2877.
- [38] Volodymyr Mnih, Koray Kavukcuoglu, David Silver, Alex Graves, Ioannis Antonoglou, Daan Wierstra, and Martin Riedmiller. 2013. Playing atari with deep reinforcement learning. *arXiv preprint arXiv:1312.5602* (2013).
- [39] J Mockus, V Tiesis, and A Zilinskas. 1978. The Application of Bayesian Methods for Seeking the Extremum. Vol. 2. *Towards Global Optimization* 2 (1978), 117–129.
- [40] Seyed-Mohsen Moosavi-Dezfooli, Alhussein Fawzi, Omar Fawzi, and Pascal Frossard. 2017. Universal Adversarial Perturbations. In *Conference on Computer Vision and Pattern Recognition*. 86–94.
- [41] Seyed-Mohsen Moosavi-Dezfooli, Alhussein Fawzi, and Pascal Frossard. 2016. Deepfool: a Simple and Accurate Method to Fool Deep Neural Networks. In *Conference on Computer Vision and Pattern Recognition*. 2574–2582.
- [42] Luis Muñoz González and Emil C Lupu. 2018. The Secret of Machine Learning. *ITNOW* 60, 1 (2018), 38–39.
- [43] Luis Muñoz-González, Battista Biggio, Ambra Demontis, Andrea Paudice, Vasin Wongrassamee, Emil C Lupu, and Fabio Roli. 2017. Towards Poisoning of Deep Learning Algorithms with Back-gradient Optimization. In *Workshop on Artificial Intelligence and Security*. 27–38.
- [44] Blaine Nelson, Marco Barreno, Fuching Jack Chi, Anthony D Joseph, Benjamin IP Rubinstein, Udum Saini, Charles A Sutton, J Doug Tygar, and Kai Xia. 2008. Exploiting Machine Learning to Subvert Your Spam Filter. *LEET* 8 (2008), 1–9.
- [45] Chris Olah, Alexander Mordvintsev, and Ludwig Schubert. 2017. Feature visualization. *Distill* 2, 11 (2017), e7.
- [46] Maxime Oquab, Leon Bottou, Ivan Laptev, and Josef Sivic. 2014. Learning and transferring mid-level image representations using convolutional neural networks. In *Proceedings of the IEEE conference on computer vision and pattern recognition*. 1717–1724.
- [47] Nicolas Papernot, Patrick McDaniel, and Ian Goodfellow. 2016. Transferability in Machine Learning: From Phenomena to Black-box Attacks using Adversarial Samples. *arXiv preprint arXiv:1605.07277* (2016).
- [48] Nicolas Papernot, Patrick McDaniel, Ian Goodfellow, Somesh Jha, Z Berkay Celik, and Ananthram Swami. 2017. Practical Black-box Attacks Against Machine Learning. In *Asia Conference on Computer and Communications Security*. 506–519.
- [49] Nicolas Papernot, Patrick McDaniel, Somesh Jha, Matt Fredrikson, Z Berkay Celik, and Ananthram Swami. 2016. The Limitations of Deep Learning in Adversarial Settings. In *European Symposium on Security and Privacy*. 372–387.
- [50] Nicolas Papernot, Patrick McDaniel, Arunesh Sinha, and Michael P Wellman. 2018. SoK: Security and Privacy in Machine Learning. In *European Symposium on Security and Privacy*. 399–414.
- [51] Andrea Paudice, Luis Muñoz-González, Andras Gyorgy, and Emil C Lupu. 2018. Detection of Adversarial Training Examples in Poisoning Attacks through Anomaly Detection. *arXiv preprint arXiv:1802.03041* (2018).
- [52] Andrea Paudice, Luis Muñoz-González, and Emil C Lupu. 2018. Label Sanitization against Label Flipping Poisoning Attacks. *Nemesis'18 Workshop on Recent Advances in Adversarial Machine Learning (ECML/PKDD)* (2018).
- [53] Ken Perlin. 1985. An Image Synthesizer. *ACM Siggraph Computer Graphics* 19, 3 (1985), 287–296.
- [54] Ken Perlin. 2002. Improved noise reference implementation. (2002). <https://mrl.nyu.edu/~perlin/noise/> Accessed: 2018-06-09.
- [55] Ken Perlin. 2002. Improving Noise. In *ACM Transactions on Graphics*, Vol. 21. 681–682.
- [56] Carl Edward Rasmussen and Christopher K. I. Williams. 2006. *Gaussian Processes for Machine Learning*. The MIT Press.
- [57] Olga Russakovsky, Jia Deng, Hao Su, Jonathan Krause, Sanjeev Satheesh, Sean Ma, Zhiheng Huang, Andrej Karpathy, Aditya Khosla, Michael Bernstein, et al. 2015. Imagenet large scale visual recognition challenge. *International Journal of Computer Vision* 115, 3 (2015), 211–252.
- [58] Joshua Saxe and Konstantin Berlin. 2015. Deep Neural Network Based Malware Detection using Two Dimensional Binary Program Features. In *Intl. Conference on Malicious and Unwanted Software (MALWARE)*. 11–20.
- [59] Joshua Saxe and Konstantin Berlin. 2017. eXpose: A character-level convolutional neural network with embeddings for detecting malicious URLs, file paths and registry keys. *arXiv preprint arXiv:1702.08568* (2017).
- [60] Bobak Shahriari, Kevin Swersky, Ziyu Wang, Ryan P Adams, and Nando De Freitas. 2016. Taking the Human Out of the Loop: A Review of Bayesian Optimization. *Proc. IEEE* 104, 1 (2016), 148–175.
- [61] David Silver, Aja Huang, Chris J Maddison, Arthur Guez, Laurent Sifre, George Van Den Driessche, Julian Schrittwieser, Ioannis Antonoglou, Veda Panneershelvam, Marc Lanctot, et al. 2016. Mastering the Game of Go with Deep Neural Networks and Tree search. *Nature* 529, 7587 (2016), 484–489.
- [62] Karen Simonyan and Andrew Zisserman. 2014. Very Deep Convolutional Networks for Large-scale Image Recognition. *arXiv preprint arXiv:1409.1556* (2014).
- [63] Jasper Snoek, Hugo Larochelle, and Ryan P Adams. 2012. Practical Bayesian Optimization of Machine Learning Algorithms. In *Advances in Neural Information Processing Systems*. 2951–2959.
- [64] Yi Sun, Xiaogang Wang, and Xiaoou Tang. 2013. Deep convolutional network cascade for facial point detection. In *Proceedings of the IEEE conference on computer vision and pattern recognition*. 3476–3483.
- [65] Christian Szegedy, Sergey Ioffe, Vincent Vanhoucke, and Alexander A Alemi. 2015. Inception-v4, Inception-Resnet and the Impact of Residual Connections on Learning. In *AAAI*, Vol. 4. 12.
- [66] Christian Szegedy, Vincent Vanhoucke, Sergey Ioffe, Jon Shlens, and Zbigniew Wojna. 2016. Rethinking the Inception Architecture for Computer Vision. In *Conference on Computer Vision and Pattern Recognition*. 2818–2826.
- [67] Christian Szegedy, Wojciech Zaremba, Ilya Sutskever, Joan Bruna, Dumitru Erhan, Ian Goodfellow, and Rob Fergus. 2013. Intriguing Properties of Neural

- Networks. *arXiv preprint arXiv:1312.6199* (2013).
- [68] Yuchi Tian, Kexin Pei, Suman Jana, and Baishakhi Ray. 2018. Deeptest: Automated testing of deep-neural-network-driven autonomous cars. In *Proceedings of the 40th international conference on software engineering*. ACM, 303–314.
  - [69] Florian Tramr, Alexey Kurakin, Nicolas Papernot, Ian Goodfellow, Dan Boneh, and Patrick McDaniel. 2018. Ensemble Adversarial Training: Attacks and Defenses. In *International Conference on Learning Representations*.
  - [70] Bichen Wu, Forrest N Iandola, Peter H Jin, and Kurt Keutzer. 2017. SqueezeDet: Unified, Small, Low Power Fully Convolutional Neural Networks for Real-Time Object Detection for Autonomous Driving.. In *CVPR Workshops*. 446–454.
  - [71] Chaowei Xiao, Jun-Yan Zhu, Bo Li, Warren He, Mingyan Liu, and Dawn Song. 2018. Spatially transformed adversarial examples. *arXiv preprint arXiv:1801.02612* (2018).
  - [72] Jason Yosinski, Jeff Clune, Yoshua Bengio, and Hod Lipson. 2014. How transferable are features in deep neural networks?. In *Advances in neural information processing systems*. 3320–3328.
  - [73] Wen Zhou, Xin Hou, Yongjun Chen, Mengyun Tang, Xiangqi Huang, Xiang Gan, and Yong Yang. 2018. Transferable Adversarial Perturbations. In *Computer Vision—ECCV 2018*. Springer, 471–486.